

# We are IntechOpen, the world's leading publisher of Open Access books Built by scientists, for scientists

6,900

Open access books available

185,000

International authors and editors

200M

Downloads

Our authors are among the

154

Countries delivered to

TOP 1%

most cited scientists

12.2%

Contributors from top 500 universities



WEB OF SCIENCE™

Selection of our books indexed in the Book Citation Index  
in Web of Science™ Core Collection (BKCI)

Interested in publishing with us?  
Contact [book.department@intechopen.com](mailto:book.department@intechopen.com)

Numbers displayed above are based on latest data collected.  
For more information visit [www.intechopen.com](http://www.intechopen.com)



---

# **Application of Different Advanced Oxidation Processes for the Degradation of Organic Pollutants**

---

Amilcar Machulek Jr., Silvio C. Oliveira,  
Marly E. Osugi, Valdir S. Ferreira, Frank H. Quina,  
Renato F. Dantas, Samuel L. Oliveira,  
Gleison A. Casagrande, Fauze J. Anaissi,  
Volnir O. Silva, Rodrigo P. Cavalcante, Fabio Gozzi,  
Dayana D. Ramos, Ana P.P. da Rosa, Ana P.F. Santos,  
Douclasse C. de Castro and Jéssica A. Nogueira

Additional information is available at the end of the chapter

<http://dx.doi.org/10.5772/53188>

---

## **1. Introduction**

Water is not only an economic, but also an increasingly important social commodity. Potable water is an essential resource for sustaining economic and social development in all sectors. A safe water supply and appropriate sanitation are the most essential components for a healthy and prosperous life. However, increases in human activities have led to exposure of the aqueous environment to chemical, microbial and biological pollutants as well as to micro-pollutants. Thus, liquid effluents containing toxic substances are generated by a variety of chemistry-related industrial processes, as well as by a number of common household or agricultural applications.

New, economically viable, more effective methods for pollution control and prevention are required for environmental protection and effluent discharge into the environment must have minimal impact on human health, natural resources and the biosphere.

Research in photochemical and photocatalytic technology is very promising for the development of viable alternatives for the treatment of polluted waters and effluents from various sources, including both industrial and domestic. Currently available chemical and photochemical technology permits the conversion of organic pollutants with a wide range of

chemical structures into substances that are less toxic and/or more readily biodegradable by employing chemical oxidizing agents in the presence of an appropriate catalyst and/or ultraviolet light to oxidize or degrade the pollutant of interest. These technologies known as advanced oxidation processes (AOP) or advanced oxidation technologies (AOT), have been widely studied for the degradation of diverse types of industrial wastewaters. These processes are particularly interesting for the treatment of effluents containing highly toxic organic compounds, for which biological processes may not be applicable unless bacteria that are adapted to live in toxic media are available. The production of powerful oxidizing agents, such as the hydroxyl radical, is the main objective of most AOP. The hydroxyl radical reacts rapidly and relatively non-selectively with organic compounds by hydrogen abstraction, by addition to unsaturated bonds and aromatic rings, or by electron transfer. In the case of persistent organic pollutants (wastes), complete decontamination may require the sequential application of several different decontamination technologies such as a pretreatment with a photochemical AOP followed by a biological or electrochemical treatment.

This chapter discusses the influence of different AOP on the degradation and mineralization of several different classes of organic pollutants such as pesticides, pharmaceutical formulations and dyes. The use of the Fenton and photo-Fenton reactions as tools for the treatment of pesticides and antineoplastic agents is presented, as well as examples of the optimization of the important parameters involved in the process such as the source of iron ions (free or complexed), the irradiation source (including the possibility of using sunlight), and the concentrations of iron ions and hydrogen peroxide. The chapter also reports the use of TiO<sub>2</sub> nanotubes obtained by electrochemical anodization, nanoparticles prepared by a molten salt technique, and Ag-doped TiO<sub>2</sub> nanoparticles as heterogeneous photocatalysts, emphasizing their potential for use in environmental applications. These catalysts were characterized by a combination of techniques, including scanning electron microscopy, elemental analysis, and energy dispersive x-ray spectroscopy.

## 2. Advanced Oxidation Processes (AOP)

AOP are specific chemical reactions characterized by the generation of chemical oxidizing agents capable of oxidizing or degrading the pollutant of interest. The efficiency of the AOP is generally maximized by the use of an appropriate catalyst and/or ultraviolet light [1-3].

In most AOP, the objective is to use systems that produce the hydroxyl radical (HO•) or another species of similar reactivity such as sulfate radical anion (SO<sub>4</sub>•<sup>-</sup>). These radicals react with the majority of organic substances at rates often approaching the diffusion-controlled limit (unit reaction efficiency per encounter). Both of these species are thus highly reactive and only modestly selective in their capacity to degrade toxic organic compounds present in aqueous solution. The principal reaction pathways of HO• with organic compounds include hydrogen abstraction from aliphatic carbon, addition to double bonds and aromatic rings, and electron transfer [4]. These reactions generate organic radicals as transient intermediates, which then undergo further reactions, eventually resulting in final products corresponding to the net oxidative degradation of the starting molecule [5].

The AOP are of two main types: homogeneous and heterogeneous processes, both of which can be conducted with or without the use of UV radiation. Thus, for example, the homogeneous process based on the reaction of  $\text{Fe}^{2+}$  with  $\text{H}_2\text{O}_2$ , known as the thermal-Fenton reaction process typically becomes more efficient for the mineralization of organic material present in the effluent when it is photocatalysed. This latter process ( $\text{Fe}^{2+}/\text{Fe}^{3+}$ ,  $\text{H}_2\text{O}_2$ , UV-Vis) is commonly referred to as the photo-Fenton reaction. Among the heterogeneous AOP, processes using some form of the semiconductor  $\text{TiO}_2$  stand out because UV irradiation of  $\text{TiO}_2$  results in the generation of hydroxyl radicals, promoting the oxidation of organic species [1,6].

## 2.1. Advances in research on AOP

AOP and their applications have attracted the attention of both the scientific community and of corporations interested in their commercialization. This can be illustrated by means of searches, in August, 2012, of the Science Finder Scholar database (version 2012). This database covers the complete text of articles/papers indexed from over 15475 international journals and 126 databases with abstracts of documents in all areas, as well as several other important sources of academic information. The results of the searches were organized as histograms to show the evolution of the number of publications (articles or patents) related to the different kinds of AOP. Figure 1 shows the results of a search using the keywords "advanced oxidation processes", which yielded approximately 840 publications and which nicely reflects the rapid growth in interest AOP, given the unique characteristics and the versatility of application of AOP.

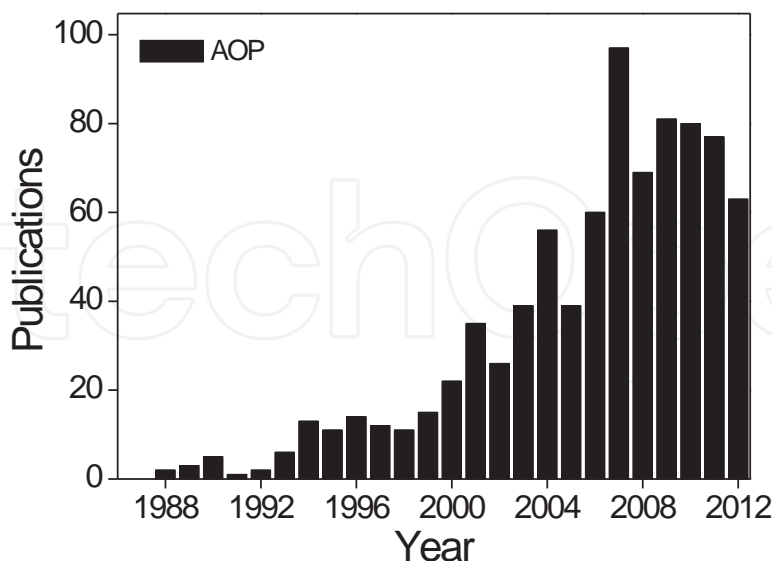


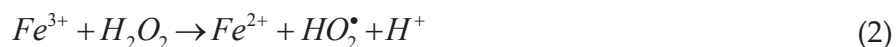
**Figure 1.** Number of publications per year indexed in the Science Finder Scholar database retrieved using the keywords "advanced oxidation processes".

## 2.2. Fenton reaction

The thermal Fenton reaction is chemically very efficient for the removal of organic pollutants. The overall reaction is a simple redox reaction in which Fe(II) is oxidized to Fe(III) and  $H_2O_2$  is reduced to the hydroxide ion plus the hydroxyl radical.



The ferric ion produced in Equation 1 can in principle be reduced back to ferrous ion by a second molecule of hydrogen peroxide:



However, this thermal reduction (Equation 2) is much slower than the initial step (Equation 1) and the addition of relatively large, essentially stoichiometric amounts of Fe(II) may be required in order to degrade the pollutant of interest [7]. Another important limitation of the Fenton reaction is the formation of recalcitrant intermediates that can inhibit complete mineralization. Despite these potential limitations, the conventional Fenton reaction has been widely used for the treatment of effluents [6, 8-11].

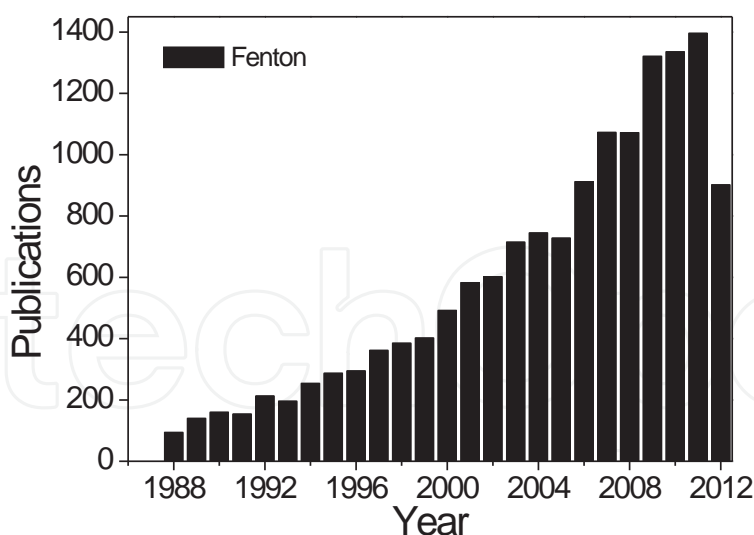


**Figure 2.** Number of publications per year indexed in the Science Finder Scholar database retrieved using the keyword "Fenton".

For the degradation of organic molecules, the optimum pH for the Fenton reaction is typically in the range of pH 3-4 and the optimum mass ratio of catalyst (as iron) to hydrogen peroxide

is 1:5 respectively [12]. One way of accelerating the Fenton reaction is via the addition of catalysts, in general from certain classes of organic molecules such as benzoquinones or dihydroxybenzene (DHB) derivatives [13,14]. It is also possible to accelerate the Fenton reaction via irradiation with ultraviolet light, a process generally known as the photo-assisted Fenton or photo-Fenton reaction, which is discussed in the following section.

Regarding the Fenton reaction, a search of Science Finder Scholar (2012) with the keyword "Fenton" without any refinements retrieved 14821 publications from 1986 to 2012. As shown in Figure 2, there is a clear upward trend in the publications, with 902 publications related to this topic being reported in just the first half of 2012.

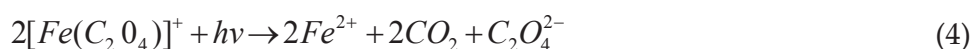
### 2.3. Photo-fenton reaction

One of the most efficient AOP is the photo-Fenton reaction ( $\text{Fe}^{2+}/\text{Fe}^{3+}$ ,  $\text{H}_2\text{O}_2$ , UV light), which successfully oxidizes a wide range of organic and inorganic compounds. The irradiation of Fenton reaction systems with UV/Vis light (250-400 nm) strongly accelerates the rate of degradation. This behavior is due principally to the photochemical reduction of Fe(III) back to Fe(II), for which the overall process can be written as:



Studies of the pH dependence of the photo-Fenton reaction have shown that the optimum pH range is ca. pH 3. Studies of the photochemistry of  $\text{Fe}(\text{OH})^{2+}$ , which is the predominant species in solution at this pH and that is formed by deprotonation of hexaaquairon(III), have shown that  $\text{Fe}(\text{OH})^{2+}$  undergoes a relatively efficient photoreaction upon excitation with UV light to produce Fe(II) and the hydroxyl radical. Therefore, irradiation of Fenton reaction systems not only regenerates Fe(II), the crucial catalytic species in the Fenton reaction, but also produces an additional hydroxyl radical, the species responsible for provoking the degradation of organic material. As a consequence of these two effects, the photo-Fenton process is faster than the conventional thermal Fenton process.

The efficiency of the photo-Fenton process can be further enhanced by using certain organic acids to complex Fe(III). Thus, for example, oxalic acid forms species such as  $[\text{Fe}(\text{C}_2\text{O}_4)]^+$ , which absorbs light as far out as 570 nm, i.e., well into the visible region of the spectrum. This species makes the photo-Fenton reaction more efficient because it absorbs a much broader range of wavelengths of light and because, upon irradiation, it efficiently decomposes (quantum yield of the order of unity) to Fe(II) and  $\text{CO}_2$ :



The use of photo-Fenton reaction has considerable advantages in practical applications. It generally produces oxidation products of low toxic, requires only small quantities of iron salt (which can be either  $\text{Fe}^{3+}$  or  $\text{Fe}^{2+}$ ) and offers the possibility of using solar radiation as the source

of light in the reaction process sunlight constitutes an inexpensive, environmentally friendly, renewable source of ultraviolet photons for use in photochemical processes.

The disadvantages of the photo-Fenton process include the low pH values required and the need for removal of the iron catalyst after the reaction has terminated. If necessary, however, the residual Fe(III) can usually be precipitated as iron hydroxide by increasing the pH. Any residual hydrogen peroxide that is not consumed in the process will spontaneously decompose into water and molecular oxygen, being thus a "clean" reagent itself. These features make homogeneous photo-Fenton based AOPs the leading candidate for cost-efficient, environmental friendly treatment of industrial effluents on a small to moderate scale [6, 15-17]. Currently much research activity is focused on attempts to develop new catalysts that function at neutral pH that do not require acidification of the effluent in order to react and that also do not require removal of the catalyst at the end of the reaction.

A search of Science Finder Scholar (2012) with the keyword "photo-Fenton" (Figure 3) showed a modest increase during the 1990s followed by a much more robust upward trend since ca. 2000.

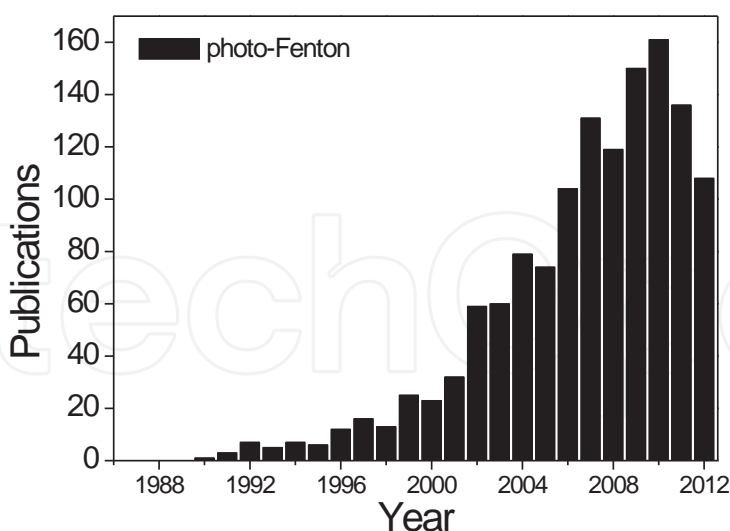


**Figure 3.** Number of publications per year indexed in the Science Finder Scholar database retrieved using the keyword "photo-Fenton".



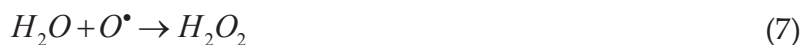
## 2.4. Ozone

Ozone is a powerful oxidizing agent with a high reduction potential (2.07V) that can react with many organic substrates [18,19]. Using ozone, the oxidation of the organic matrix can occur via either direct or indirect routes [20,21]. In the direct oxidation route, ozone molecules can react directly with other organic or inorganic molecules via electrophilic addition. The electrophilic attack of ozone occurs on atoms with a negative charge (N, P, O, or nucleophilic carbons) or on carbon-carbon, carbon-nitrogen and nitrogen-nitrogen pi-bonds [22,23]. Indirectly, ozone can react via radical pathways (mainly involving HO•) initiated by the decomposition of ozone.

A process that employs ozone is only characterized as an AOP when the ozone decomposes to generate hydroxyl radicals (Equation 5), a reaction that is catalyzed by hydroxide ions (OH<sup>-</sup>) in alkaline medium or by transition metal cations [18,24,25].



The efficiency of ozone in degrading organic compounds is improved when combined with H<sub>2</sub>O<sub>2</sub>, UV radiation or ultrasound. The initial step in the UV photolysis of ozone is dissociation to molecular oxygen and an oxygen atom (Equation 6), which then reacts with water to produce H<sub>2</sub>O<sub>2</sub> (Equation 7):



In a second photochemical step (Equation 8), H<sub>2</sub>O<sub>2</sub> photodissociates into the active species, two hydroxyl radicals:



The O<sub>3</sub>/UV process has been employed commercially to treat ground water contaminated with chlorinated hydrocarbons, but cannot compete economically with the H<sub>2</sub>O<sub>2</sub>/UV process. A major problem with the use of ozone for water treatment is bromine formation in waters containing bromide ion. Strategies such as addition of H<sub>2</sub>O<sub>2</sub> (O<sub>3</sub>/H<sub>2</sub>O<sub>2</sub>) can reduce bromine formation and assure the suitability of ozone for treating drinking and wastewater [26].

A search of the Science Finder Scholar database retrieved using only the keyword "ozone" retrieved, as expected, an enormous number of publications, nearly 130,000. Refinement with the additional keyword "degradation" reduced this to 3057 publications, which is a significant number when compared with other AOPs, especially in recent years (Figure 4).



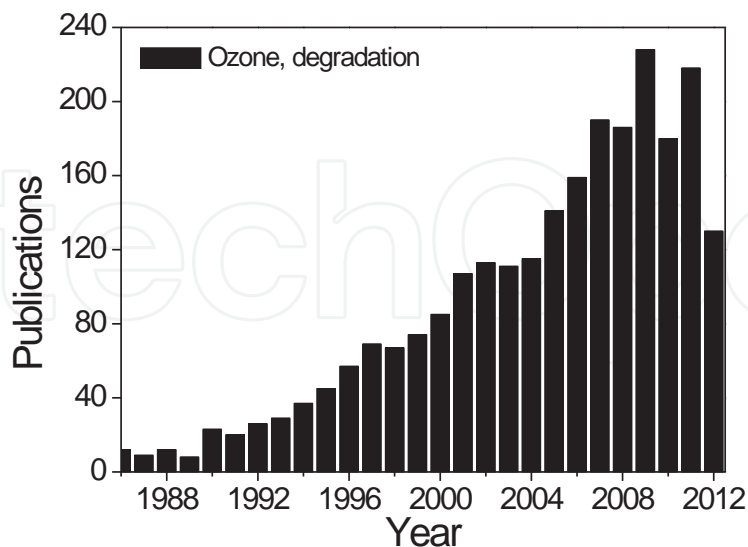


**Figure 4.** Number of publications per year indexed in the Science Finder Scholar database retrieved using the keywords "ozone" and "degradation".

## 2.5. Heterogeneous AOP

Another important class of AOP is based on the use of solid semiconductors as heterogeneous catalysts for the mineralization of organic compounds. In this type of photocatalysis, an electron in the valence band of the semiconductor ( $\text{CdS}$ ,  $\text{TiO}_2$ ,  $\text{ZnO}$ ,  $\text{WO}_3$ , etc.) is promoted into the conduction band upon excitation. The electron in the conduction band typically reacts with  $\text{O}_2$ , while the hole in the valence band can react with an adsorbed pollutant or oxidize water to produce a surface-bound  $\text{HO}^\bullet$  radical [2].

According to Alfano and coworkers [27], the anatase form of titanium dioxide ( $\text{TiO}_2$ ) is the material most indicated for use in photocatalytic water treatment, considering aspects such as toxicity, resistance to photocorrosion, availability, catalytic efficiency and cost. Using  $\text{TiO}_2$  as the semiconductor, the photocatalysis is based on the activation of anatase by light [28]. The band gap or energy difference between the valence and conduction bands of anatase is 3.2 eV. Thus, UV light of wavelength shorter than 390 nm is capable of exciting an electron ( $e^-$ ) from the valence to the conduction band.



An important feature of  $\text{TiO}_2$  photocatalysis is the very high oxidation potential of the holes left in the valence band (3.1 eV at pH 0), making it possible for photoexcited  $\text{TiO}_2$  to oxidize most organic molecules.

The electron ( $e^-$ ) and hole ( $h^+$ ) pair produced by absorption of UV light can migrate to the surface of the anatase particle, where they react with adsorbed oxygen, water, hydroxide ion or organic species via electron transfer reactions. Both water and hydroxide ion can act as electron donors to the holes ( $h^+$ ) of the catalyst [27,29], generating hydroxyl radicals, as shown by Equations 10 and 11.



When dissolved molecular oxygen is present or is deliberately added to the medium, it can act as an acceptor of the electron in the conduction band, generating the superoxide radical (Equation 12) and triggering a series of reactions that can lead to the formation of hydroxyl radicals [30,31].

Alternatively, one can increase the oxidative efficiency of  $TiO_2$  photocatalysis by adding  $H_2O_2$ . The electrons in the conduction band then reduce the added  $H_2O_2$  to  $HO^\bullet$  and  $HO^-$  [32], according to Equation 13.



The use of  $TiO_2$  also makes it possible to degrade organic molecules that are resistant to oxidation, since they can potentially be reduced by the electrons in the conduction band.

$TiO_2$  photocatalysis has a number of important advantages in relation to other AOP and, in some aspects, even some biological treatments. In particular, unlike other AOP, the  $TiO_2$ /UV system can be employed to treat pollutants in the gas phase, as well as in solution. In addition,  $TiO_2$  has a relatively low cost, is essentially insoluble in water and biologically and chemically inert. Moreover, it can be used to treat effluents containing a wide range of concentrations of pollutants, in particular very low concentrations. Solar radiation can be used to activate the catalyst; and the excellent mineralization efficiency is observed for organochlorine compounds, chlorophenols, nitrogen-containing pesticides, aromatic hydrocarbons, dioxins, carboxylic acids, etc. The principle limitations of  $TiO_2$  photocatalysis in practical applications are the low quantum efficiency of the process and the limited depth of penetration of the incident radiation into suspensions of  $TiO_2$ , due to the strong scattering of light by the opaque white catalyst particles. Incrustation of the reactor walls with catalyst can also reduce the amount of incident light. Batch reactors also require additional unit operations in order to physically separate the catalyst from the solution at the end of the irradiation for recycling. Although substantial progress has been made in developing larger-scale reactors for carrying

out heterogeneous photochemical reactions, much work remains to be done before  $\text{TiO}_2$  photocatalysis becomes a generally applicable technique.

Figure 5 shows the evolution of publications related to heterogeneous photocatalysis by  $\text{TiO}_2$ , reflecting the potential for application of this technology on an industrial scale.

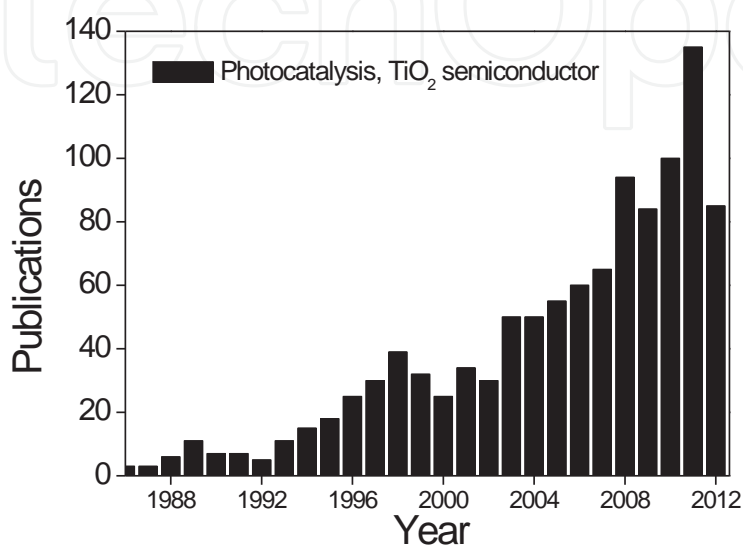


**Figure 5.** Number of publications per year indexed in the Science Finder Scholar database retrieved using the keywords "photocatalysis" and " $\text{TiO}_2$  semiconductor".

### 3. Applications

In this section, several applications of homogeneous and heterogeneous AOP are discussed, focusing on the degradation and mineralization of organic pollutants such as pesticides, pharmaceutical formulations and dyes.

#### 3.1. Homogeneous AOP applied to degradation of the herbicide chlorimurom-ethyl and the antineoplastic agent mitoxantrone

The use of the thermal Fenton and the photo-Fenton reactions for the treatment of the pesticide chlorimurom-ethyl (CE) and the antineoplastic agent mitoxantrone (MTX) is described here, along with the optimization of the parameters involved in these processes, including the sources of iron (free or complexed) and irradiation (lamp or possibility of using sunlight) and the concentrations of iron and hydrogen peroxide, etc. Ozone and ozone combined with UV and  $\text{H}_2\text{O}_2$  were also used as alternative treatments of these pesticides.

### 3.1.1. Degradation of Chlorimurom-Ethyl (CE)

The thermal Fenton, photo-Fenton and ozonation processes were applied for the degradation of a commercial preparation of chlorimurom-ethyl (CE, Figure 6), a compound belonging to the class of sulfonylurea herbicides. This herbicide, widely used in the cultivation of soybeans, may persist in the environment and has residual phytotoxicity [33].

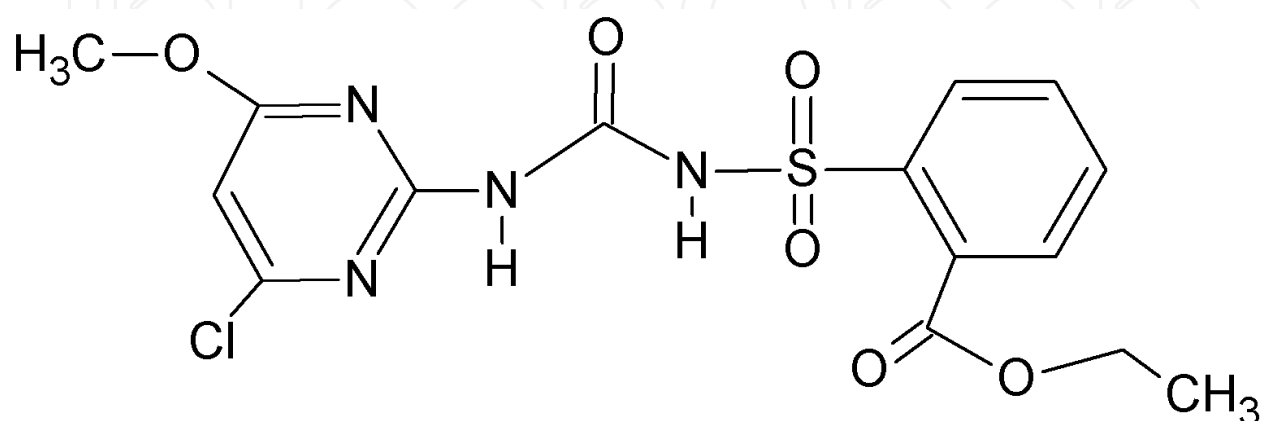


**Figure 6.** Molecular structure of Chlorimurom-ethyl (CE).

Experiments were performed in a photochemical reactor (1.0 L) equipped with a high pressure mercury lamp (125 W) coupled to a reservoir (2.0 L) via a recirculation pump. The photo-Fenton degradation was influenced by the initial concentrations of  $\text{H}_2\text{O}_2$  and  $\text{Fe}^{2+}$ . Experiments were performed with different  $\text{H}_2\text{O}_2$  concentrations, ranging from 17 to 103  $\text{mmol L}^{-1}$ , maintaining the  $\text{Fe}^{2+}$  concentration constant at 0.33  $\text{mmol L}^{-1}$ . Subsequently, the  $\text{H}_2\text{O}_2$  concentration was fixed at 68.4  $\text{mmol L}^{-1}$ , the value that gave the best mineralization, and the  $\text{Fe}^{2+}$  concentrations were varied from 0.20 to 1.0  $\text{mmol L}^{-1}$ . The extent of mineralization of the organic material, expressed as the percentage of removal of the total organic carbon (TOC), ranged from 84% to 95%. Since the quantity of  $\text{Fe}^{2+}$  had only a small effect on CE removal, a concentration of  $\text{Fe}^{2+}$  of 0.20  $\text{mmol L}^{-1}$  was used in subsequent experiments. In all cases, the extent of mineralization was higher than the percentage of degradation of CE (82-87%) determined by HPLC. This particularity reflects the fact that a commercial formulation of CE was employed in the experiments. Thus, a solution of this formulation in water that contained 30  $\text{mg L}^{-1}$  of CE contained 65  $\text{mg L}^{-1}$  of total organic carbon. Therefore, it can be concluded that the other organic compounds present in the composition react somewhat better with  $\text{HO}^\bullet$  than CE.

The effect of UV radiation on this optimized reaction system was used to compare the efficiencies of the thermal Fenton and photo-Fenton reactions for the mineralization of CE (Figure 7) with each other and with those of several other homogeneous AOP. Under direct photolysis there was no significant mineralization. Less than 20% TOC removal was obtained at the end of the thermal Fenton treatment. However, a considerable increase in mineralization was observed when the Fenton system was irradiated with UV light. Monitoring CE removal rather than TOC showed that both the thermal Fenton reaction and the photo-Fenton reactions

caused extensive degradation of the target compound. Therefore, in the photo-Fenton process, UV radiation makes a significant contribution to both mineralization and CE removal.

Normative Instruction nº 2, published on January 3, 2008, by the Brazilian Ministry of Agriculture (MAPA) [34], regulates the practice in Brazil for treatment of pesticide residues in effluents generated by agricultural aviation companies. The Ministry recommends ozonation for a minimum of six hours using a system with a minimum capacity for producing one gram of ozone per hour for each charge of four hundred and fifty liters of pesticide residue derived from washing and cleaning of aircraft equipment [34]. To verify the efficiency of this system for the mineralization of CE-contaminated water, the samples were treated with ozone alone and with ozone in combination with UV light and  $\text{H}_2\text{O}_2$ . Although oxidation of CE was very fast with all the ozonation methods studied, the use of ozone alone proved to be of limited utility with regard to the mineralization of the organic content of CE-contaminated waters. The combination of  $\text{O}_3/\text{UV}/\text{H}_2\text{O}_2$  did, however, achieve a high extent of mineralization (80%), indicating that the mineralization of the organic content is mediated by the  $\text{HO}^\bullet$  radical.

When compared to the other systems studied, the photo-Fenton system showed the best results, with mineralization exceeding 85%, making it the preferred technique for the treatment of wastewater containing this pesticide.

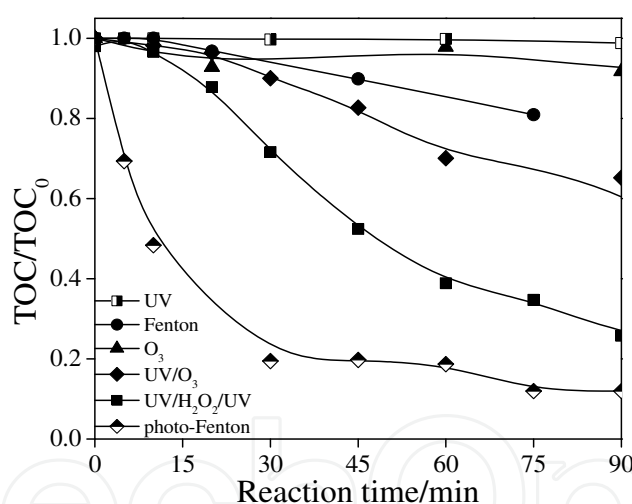


**Figure 7.** Comparison of the efficiencies of mineralization of a commercial formulation of CE in aqueous solution by the different AOP.  $[\text{CE}]_0 = 0.060 \text{ mmol L}^{-1}$ ;  $[\text{TOC}]_0 = 65 \text{ mg L}^{-1}$ ; when present,  $[\text{Fe}^{2+}] = 0.2 \text{ mmol L}^{-1}$ ,  $[\text{H}_2\text{O}_2] = 68.4 \text{ mmol L}^{-1}$  and  $[\text{O}_3] = 25 \text{ mg mL}^{-1}$ .

### 3.1.2. Degradation of Mitoxantrone (MTX)

Antineoplastic agents (drugs employed in cancer chemotherapy) are pollutants due their mutagenic, carcinogenic, and genotoxic potential, even at trace levels [35]. The AOP selected for degradation of the antineoplastic drug mitoxantrone (MTX), Figure 8 [36], were the photo-Fenton (with  $\text{Fe}^{2+}$ ,  $\text{Fe}^{3+}$ , and potassium ferrioxalate -  $\text{K}_3(\text{FeOx})$  - as iron sources), solar photo-Fenton, Fenton and  $\text{UV}/\text{H}_2\text{O}_2$  reactions. The MTX degradation experiments were carried out

using an annular glass photochemical reactor (working volume, 1 L) and a quartz tube for introduction of the radiation source (a 125 W mercury vapor lamp).

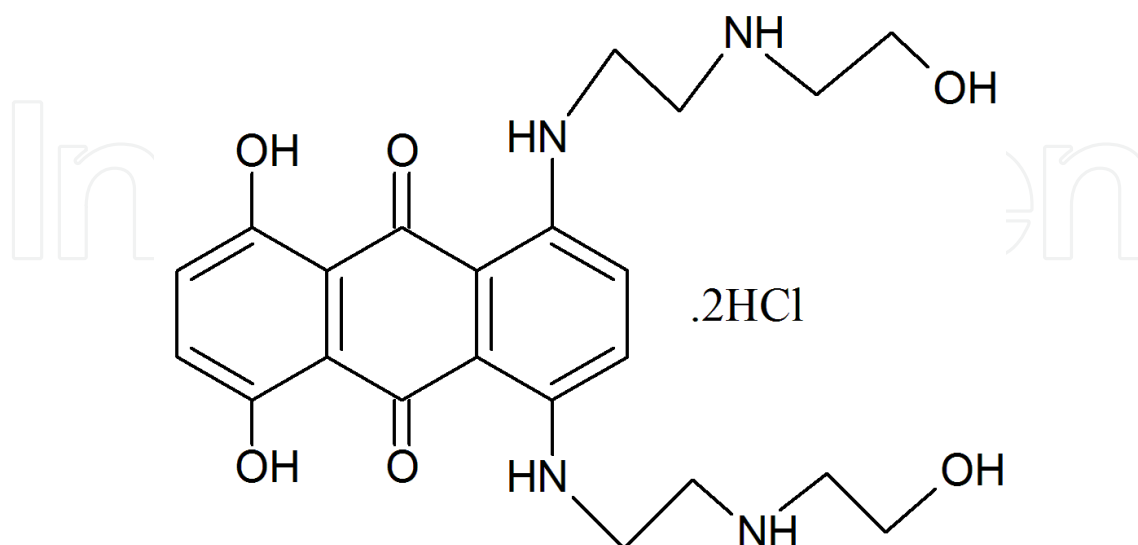


**Figure 8.** Molecular structure of Mitoxantrone.

Degradation of MTX by the photo-Fenton process was investigated with several different concentrations of Fe(II) (0.54, 0.27, and 0.13 mmol L<sup>-1</sup>) and H<sub>2</sub>O<sub>2</sub> (4.0, 9.4, and 18.8 mmol L<sup>-1</sup>). The results showed a low removal of TOC, with a mineralization of only 14-35%. One explanation for this low efficiency is that MTX has nitrogen and oxygen atoms that might serve as complexation sites for iron(III), making it unavailable for participation in the Fenton reaction. The possibility of complexation between MTX and iron(III) was investigated by spectrophotometric measurements. Indeed, addition of Fe(NO<sub>3</sub>)<sub>3</sub> to solutions of MTX caused significant spectral changes, including a shift and a decrease in the absorbance of the long-wavelength absorption band (608-658 nm) of the drug. Spectrophotometric titrations suggested that the complex has a 2:1 Fe<sup>3+</sup>:MTX stoichiometric ratio with a complexation constant (*K*) of 1.47 × 10<sup>4</sup> M<sup>-2</sup> indicative of a high affinity of MTX for Fe<sup>3+</sup>.

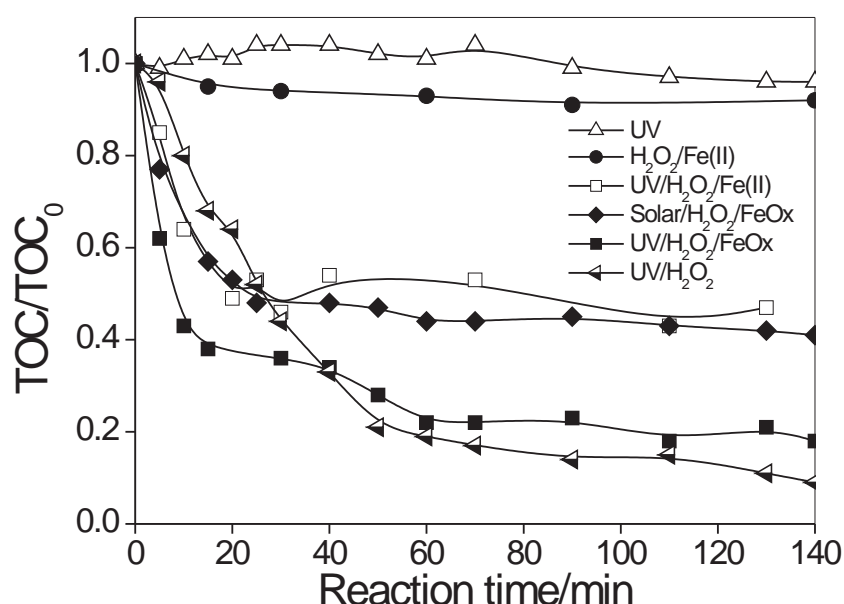
In order to minimize the effects of the complexation of Fe(III) by MTX, the use of more stable, but photoactive iron complexes as the source of iron in the degradation process was examined. One such complex is potassium ferrioxalate K<sub>3</sub>(FeOx). This complex is often employed because of its high quantum efficiency of photodecomposition and strong absorption in the UV-visible region (up to 500 nm), compatible with the use of solar irradiation in a K<sub>3</sub>(FeOx) - mediated photo-Fenton process [37].

Figure 9 compares the efficiencies of several different AOP for the degradation of MTX. The photo-Fenton process employing K<sub>3</sub>(FeOx) and the UV/H<sub>2</sub>O<sub>2</sub> process were the most efficient for mineralizing MTX, with 82% and 90% total organic carbon removal, respectively. Total degradation of MTX was observed in the thermal Fenton process, but only 65% degradation of MTX occurred under UV irradiation alone; However, TOC data show that there was no appreciable mineralization of MTX under direct photolysis and in the thermal Fenton reaction,



even after long treatment periods, whereas the photo-Fenton reaction using solar irradiation led to a TOC removal of 59%.

Although the UV/H<sub>2</sub>O<sub>2</sub> process is usually slower than the photo-Fenton process, due to the complexation of MTX with Fe(III) in the latter, the UV/H<sub>2</sub>O<sub>2</sub> process proved to be more efficient in this case. To corroborate this, the amount of photogenerated Fe(II) was quantified during the irradiation of ferric ions [Fe(NO<sub>3</sub>)<sub>3</sub>] and ferrioxalate in the presence of MTX. In the presence of MTX, the photoreduction of Fe(III) generated only 75  $\mu\text{mol L}^{-1}$  of Fe(II), while irradiation of ferrioxalate generated 285  $\mu\text{mol L}^{-1}$  of Fe(II) under the same experimental conditions. This conclusively shows that MTX inhibits the photochemical step of the photo-Fenton reaction, making the overall process substantially less efficient.



**Figure 9.** Comparison of the mineralization of aqueous MTX solutions (0.077 mmol L<sup>-1</sup>) by different AOP (0.54 mmol L<sup>-1</sup> iron source and 18.8 mmol L<sup>-1</sup> H<sub>2</sub>O<sub>2</sub>, when present).

Cytotoxicity evaluation of the solution during treatment by an AOP is a very important since the intermediates and by-products formed during the oxidation of the organic material can be more toxic than the initial target compound. Cytotoxicity tests were performed using NIH/3T3 mouse embryonic fibroblast cells. The concentration (IC<sub>50</sub>) for inhibition of growth by MTX was 3.29  $\mu\text{g mL}^{-1}$ , demonstrating its toxicity to NIH/3T3 cells. In contrast, 100% growth of NIH/3T3 cells was observed in similar tests on aliquots of solutions of MTX that had been degraded by the H<sub>2</sub>O<sub>2</sub>/UV and photo-Fenton (UV/H<sub>2</sub>O<sub>2</sub>/K<sub>3</sub>(FeOx)) processes, indicating an absence of toxic effects. Thus, these two AOP, which degraded MTX completely and exhibited the best mineralizations of the drug, generated no toxic by-products, confirming the potential of both of these processes for the removal of MTX from aqueous solution.



### 3.2. Preparation of TiO<sub>2</sub> semiconductors and their application in the heterogeneous photocatalysis of methyl viologen, methylene blue and xyldine

TiO<sub>2</sub> is an important, widely studied photocatalytic material [38]. Several samples of TiO<sub>2</sub> are commercially available, but Evonik (Degussa) P-25 (70% anatase and 30% rutile) is the most popular and, in most cases, gives the best results. However, different methods such as sol-gel process [39-41], electrochemical anodization [42], and molten-salt synthesis [43] can be used to prepare TiO<sub>2</sub> in the form of powders, nanoparticles, thin film, nanotubes, etc. This section considers heterogeneous photocatalysis employing TiO<sub>2</sub> in the forms of nanotubes obtained by electrochemical anodization, of nanoparticles prepared by sol-gel or molten salt techniques, and of Ag-doped TiO<sub>2</sub> nanoparticles. These catalysts were characterized by a series of techniques, including scanning electron microscopy, elemental analysis, energy dispersive x-ray spectroscopy, etc. and were applied for the degradation of a herbicide and a dye.

TiO<sub>2</sub> prepared by the sol-gel process (acid hydrolysis of titanium(IV) isopropoxide) was used for the photocatalytic degradation of the herbicide methyl viologen (MV<sup>2+</sup>, Figure 10), which is widely employed in over 130 countries on crops of rice, coffee, sugar cane, beans, and soybeans, among others [44], despite a high power of intoxication. The performance under irradiation of nanoparticles of TiO<sub>2</sub> prepared by the sol-gel technique (TiO<sub>2</sub> SG) was compared to TiO<sub>2</sub> SG doped with Ag (0.5%-4.0%), and to undoped and doped TiO<sub>2</sub> P25. The materials were characterized by thermogravimetric analysis, X-ray diffraction, surface area, infrared spectroscopy, scanning electron microscopy and energy dispersive spectroscopy. X-Ray diffraction analysis showed that TiO<sub>2</sub> synthesized by the sol-gel method is similar to TiO<sub>2</sub> P25 with both anatase and rutile peaks, but with a lower crystallinity and an increase in the surface area compared to P25. The surface area of TiO<sub>2</sub> SG, determined experimentally by BET, was 71.21 m<sup>2</sup> g<sup>-1</sup>, 1.5 times larger than TiO<sub>2</sub> P25 (46.18 m<sup>2</sup> g<sup>-1</sup>). The doping with Ag influenced the values of the band gap energy ( $E_{\text{gap}}$ ), determined by diffuse reflectance spectroscopy. Higher percentages of Ag resulted in a decrease the  $E_{\text{gap}}$  value, shifting the light absorption to the visible region. Additionally, energy dispersive spectroscopic analysis confirmed the presence of Ag in the doped materials. Scanning electron microscopic (SEM) analysis (Figure 11) indicated that silver changed the oxide morphology, depending on the amount. In materials with 0.5% (Figure 11 A) and 1.0% of Ag (Figure 11B), the agglomerates were larger, while in samples with 2.0% (Figure 11C) and 4.0% (Figure 11D) the particles were smaller and more well-defined. This indicates that the presence of larger quantities of silver in the sol-gel oxide modified the material surface, making it more uniform.

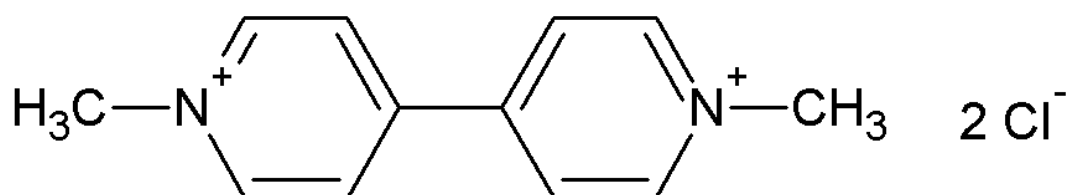


**Figure 10.** Molecular structure of Methyl Viologen.

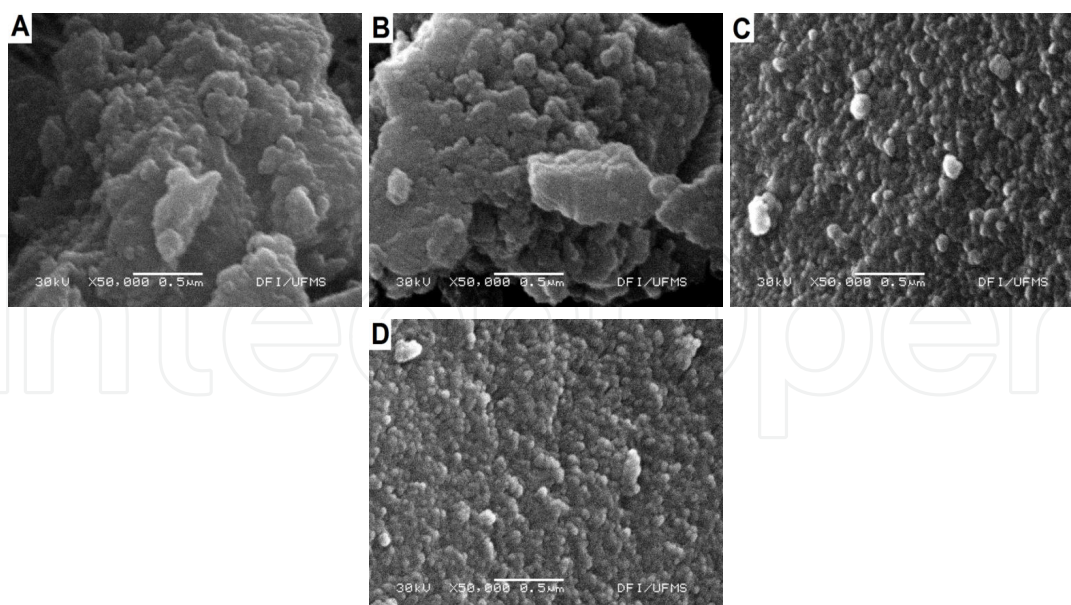


**Figure 11.** Scanning electron micrographs of: (A) TiO<sub>2</sub> SG 0.5% Ag; (B) TiO<sub>2</sub> SG 1.0% Ag; (C) TiO<sub>2</sub> SG 2.0% Ag; (D) TiO<sub>2</sub> SG 4.0% Ag.

Laser flash photolysis is a technique for producing and investigating excited states and transient reaction intermediates and the kinetics of photochemical reactions. The photocatalytic reduction of MV by TiO<sub>2</sub> or by Ag-doped TiO<sub>2</sub> (2%) in the presence and absence of sodium formate was investigated via the formation of MV•<sup>+</sup> at different initial concentrations of MV<sup>2+</sup> (0.05, 0.07, 0.1, 0.15 and 0.2 mmol L<sup>-1</sup>), monitoring the transient absorption of MV•<sup>+</sup> at 605 nm [45]. As reported by Tachikawa et al. [45], the transient absorption decays by first order kinetics. The bimolecular electron transfer rate constants in the absence and presence of sodium formate, listed in Table 1, were obtained from linear plots of the observed first-order rate constants versus the concentrations of MV<sup>2+</sup>. In the presence of sodium formate there is an increase in electron transfer constant for all photocatalysts analyzed; according Tachikawa et al [45], this occurs because the initial oxidation of organic additives, such as sodium formate, generates the CO<sub>2</sub>•<sup>-</sup> radical, which has strong reducing power and can easily reduce other substrates. There is an increase in the electron transfer rate constants in the presence of sodium formate and in the presence of silver, demonstrating the improved efficiency of the oxidation/reduction in the presence of the metal.

	Absence of NaHCO <sub>2</sub>	Presence of NaHCO <sub>2</sub>
TiO <sub>2</sub> P25	$5.4 \times 10^9 \text{ M}^{-1}\text{s}^{-1}$	$6.0 \times 10^9 \text{ M}^{-1}\text{s}^{-1}$
TiO <sub>2</sub> P25 2.0% Ag	$6.5 \times 10^9 \text{ M}^{-1}\text{s}^{-1}$	$8.0 \times 10^9 \text{ M}^{-1}\text{s}^{-1}$
TiO <sub>2</sub> SG	$3.2 \times 10^9 \text{ M}^{-1}\text{s}^{-1}$	$3.6 \times 10^9 \text{ M}^{-1}\text{s}^{-1}$
TiO <sub>2</sub> SG 2.0% Ag	$4.5 \times 10^9 \text{ M}^{-1}\text{s}^{-1}$	$6.6 \times 10^9 \text{ M}^{-1}\text{s}^{-1}$

**Table 1.** Electron transfer rate constants for MV<sup>2+</sup> in the presence of the different TiO<sub>2</sub> photocatalysts.

To test the photocatalytic activity of the oxides,  $MV^{2+}$  photodegradation experiments were performed. The amount of herbicide solution treated was 500 mL and herbicide concentration was determined by spectrophotometric analysis at 250 nm. Titanium dioxide synthesized by the sol-gel method (Figure 12B) had a lower rate of degradation than  $TiO_2$  P25 (Figure 12A). This difference can be attributed to several factors, including the preparation method, crystal structure, surface area, size distribution and porosity. Although the sol-gel oxide had a higher surface area, it contained non-uniform particles of different sizes and therefore had a lower porosity than  $TiO_2$  P25. The oxides synthesized with 2.0% silver showed improved photocatalytic activity for degradation of  $MV$ . However, in the presence of oxide doped with 4.0% silver, there was an inhibition of the photocatalytic process, probably due to the excessive amount of silver, which occupied most of the active sites of the catalyst.

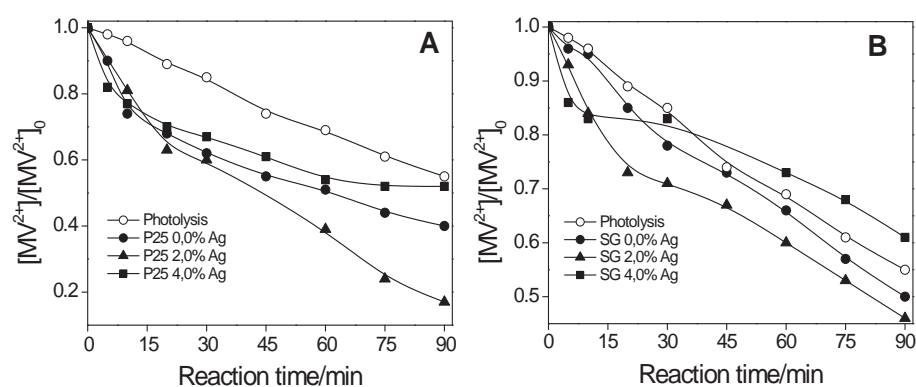
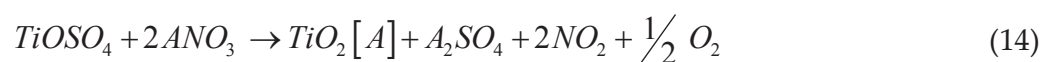


**Figure 12.** Results of  $MV^{2+}$  ( $0.2 \text{ mmol L}^{-1}$ ) degradation by heterogeneous photocatalysis ( $0.5 \text{ g}$  of photocatalyst) with (A)  $TiO_2$  P25 and (B)  $TiO_2$  SG.

An alternative method for preparing  $TiO_2$  is via molten-salt synthesis. This approach employs an eutectic mixture of salts, for example  $NaCl/KCl$  or  $NaNO_3/KNO_3$  in the desired proportion, together with other reagents (oxalates or metals oxides). Molten-salt synthesis [43] was used to prepare  $TiO_2$  using  $TiOSO_4 \cdot xH_2O \cdot xH_2SO_4$  as the Ti precursor with a melt phase of either  $NaNO_3$  or  $KNO_3$ . The synthesis reaction occurs according to Equation 14.



where the symbol  $[A]$  indicates the alkali metal cation used in the molten salt ( $[Na]$  or  $[K]$ ).

The oxides synthesized in this manner were characterized by X-ray diffraction and diffuse reflectance spectroscopy. The X-ray diffraction diffractograms (Figure 13) show only the presence of the anatase phase for both oxides synthesized by the molten-salt method. The

$E_{\text{gap}}$  values for  $\text{TiO}_2[\text{K}]$  (3.13 eV) and  $\text{TiO}_2[\text{Na}]$  (3.15 eV) were similar to that of P25 (3.13 eV), as expected.

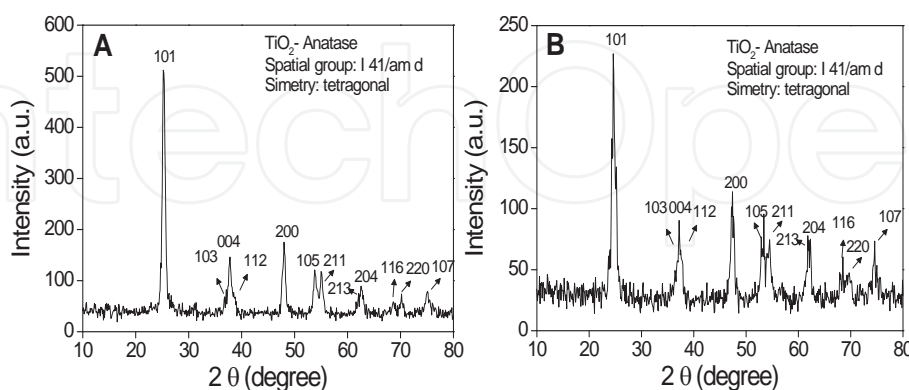


**Figure 13.** X-ray diffractograms of  $\text{TiO}_2$  synthesized by the molten salt method: (A) in  $\text{NaNO}_3$  and (B) in  $\text{KNO}_3$ .

The morphologies of the oxides, observed by SEM (Figure 14), exhibited different forms of agglomeration, presumably due to an influence of the alkaline metal nitrate molten salt used in the synthesis.

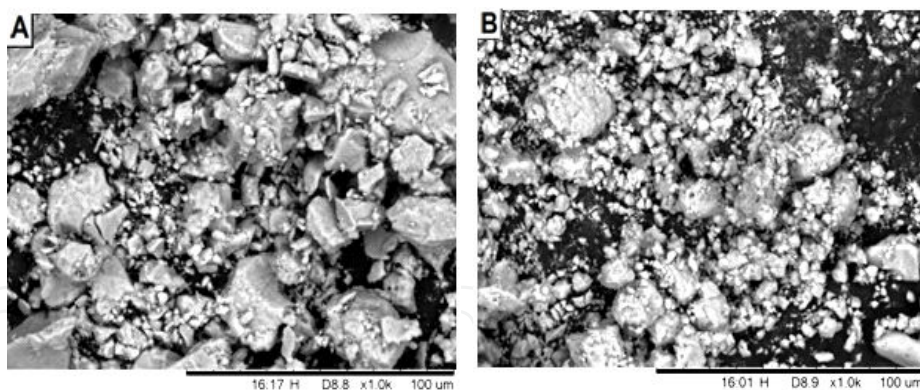


**Figure 14.** Scanning electron micrographs of (A)  $\text{TiO}_2[\text{K}]$ ; (B)  $\text{TiO}_2[\text{Na}]$ .

In order to evaluate the photocatalytic activities of the synthesized oxides, they were used for the photodegradation of the dye methylene blue (MB, Figure 15). Although MB is not considered to be a very toxic dye, it can cause harmful effects on living beings. After inhalation, symptoms such as difficulty in breathing, vomiting, diarrhea and nausea may occur in humans [46]. The degradation of MB was carried out in aqueous solution in a 400 mL reactor with an 80 W mercury vapor lamp as the irradiation source. The concentration of MB was determined from its absorption at 654 nm.

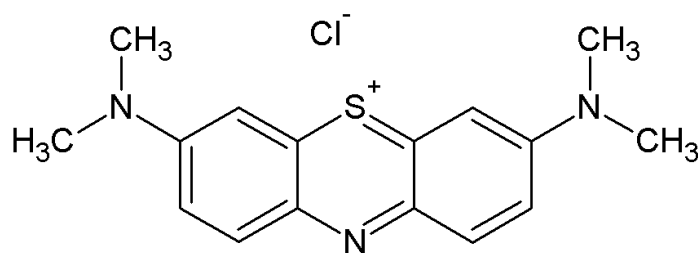


**Figure 15.** Molecular structure of Methylene Blue.

Figure 16 compares the degradation of MB using the two catalysts synthesized by the molten-salt method.  $\text{TiO}_2[\text{K}]$  produced a net degradation efficiency of 99%. In contrast,  $\text{TiO}_2[\text{Na}]$  degraded only 61% of MB. The lower rate of degradation of MB by  $\text{TiO}_2[\text{Na}]$  and the lower overall efficiency may be related to the differences in aggregation observed in the SEM images of the two oxides (Figure 14). On the basis of these results,  $\text{TiO}_2[\text{K}]$  obtained by the molten salt method would appear to be a promising alternative material for the catalytic photodegradation of organic dyes like MB.

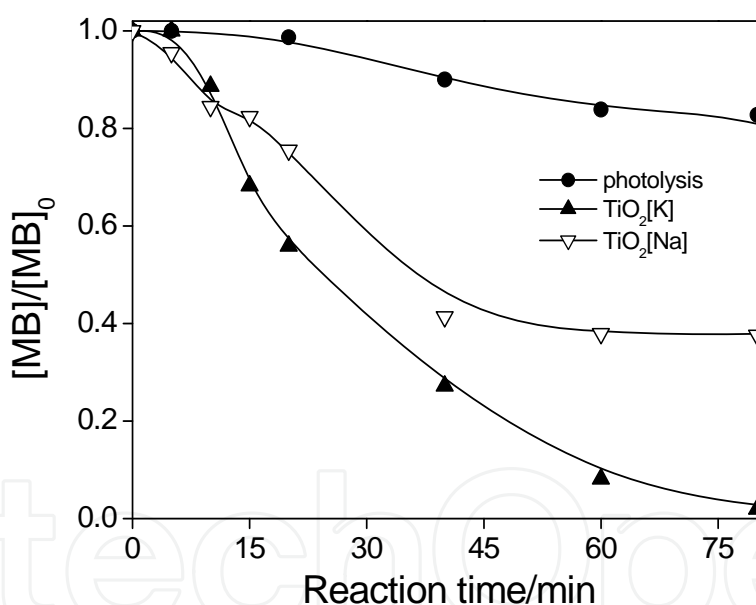


**Figure 16.** Degradation of MB ( $0.40 \text{ mmol L}^{-1}$ ) by heterogeneous photocatalysis using  $\text{TiO}_2$  ( $0.5 \text{ g L}^{-1}$ ) synthesized by the molten salt method.

$\text{TiO}_2$  nanotubes have been subject of several recent studies due to their unique electronic transport properties and their mechanical strength, large surface area and well-defined geometry, which improve their performance in many applications compared to other forms of titanium dioxide. Several studies have reported that highly ordered and uniform  $\text{TiO}_2$  nanotubes can be easily obtained using anodization in titanium fluoride [42,47]. The formation of  $\text{TiO}_2$  nanotubes by electrochemical anodization is based on a competition between the anodic oxide formation and its dissolution as a soluble complex fluoride.



Ti/TiO<sub>2</sub> electrodes (4 × 2.8 cm) were prepared by anodization of Ti foil using an applied voltage of 20 V in 0.15 mol L<sup>-1</sup> NH<sub>4</sub>F in glycerol (10% H<sub>2</sub>O). Self-assembly of nanotubular TiO<sub>2</sub> arrays can be seen on films of Ti obtained under these anodization conditions (Figure 17). The average internal diameter of the nanotubes was 66 nm.

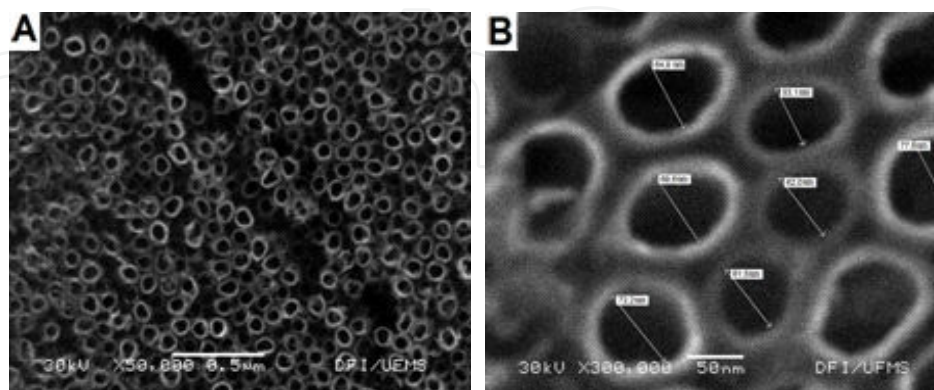


**Figure 17.** Scanning electron micrographs of TiO<sub>2</sub> nanotubes prepared on a Ti film in 0.15 mol L<sup>-1</sup> NH<sub>4</sub>F in glycerol (10% H<sub>2</sub>O) at a potential of 20 V. (A) TiO<sub>2</sub> nanotubes, (B) diameters of the nanotubes.

The photoelectrocatalytic activity of the Ti/TiO<sub>2</sub> electrodes was evaluated by linear voltammetric scans in the potential range of -0.4 to 0.7 V under UV irradiation. The photoanodic current flow arises from the photooxidation of adsorbed water molecules or hydroxyl groups on the titania surface (Figure 18).

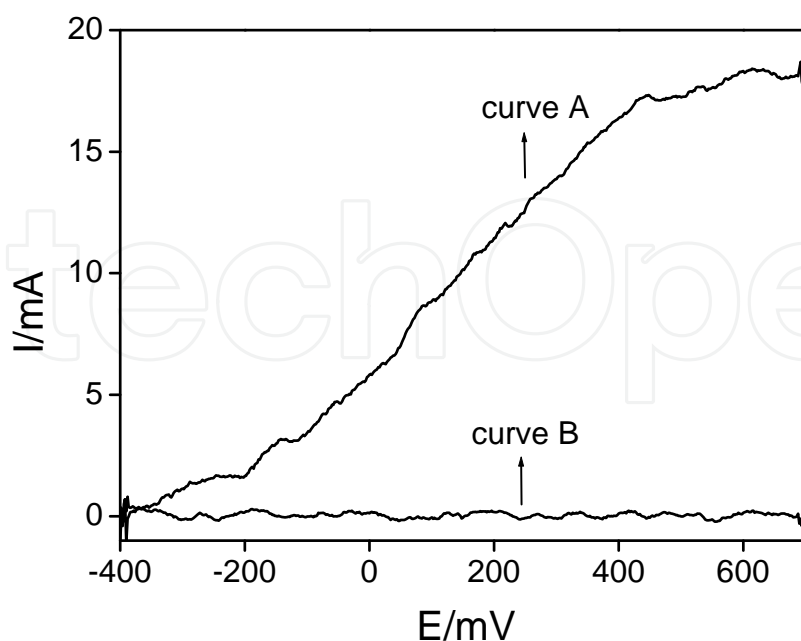


**Figure 18.** Linear-sweep photovoltammograms for TiO<sub>2</sub> nanotubes on a Ti film in 0.1 mol L<sup>-1</sup> Na<sub>2</sub>SO<sub>4</sub> (curve A) under UV illumination and in the dark (curve B). Scan rate: 5 mV s<sup>-1</sup>.

Initial studies of photoelectrocatalytic oxidation employing these electrodes was carried out using 2,4 xylidine (Figure 19) as the model pollutant. In  $0.1 \text{ mol L}^{-1} \text{ Na}_2\text{SO}_4$  supporting electrolyte applying a potential of 0.6 V, a TOC removal of 62% was obtained.

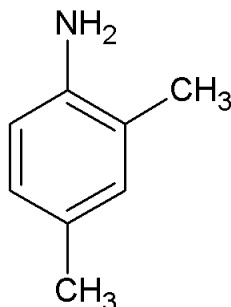


**Figure 19.** Molecular structure of 2,4-Xylidine.

## 4. Conclusion

Although there has been a considerable increase in research activity related to advanced oxidation processes (AOP) since 2000, a number of significant challenges must still be overcome to make AOP generally applicable for the treatment of polluted waters and effluents. AOP involving both homogeneous and heterogeneous catalysis have shown good results for degradation of pollutants leading to efficient mineralization. The use of  $\text{TiO}_2$  nanoparticles and nanotubes as the photocatalyst have been shown to be viable alternatives for the photodegradation of methylene blue (MB) and for the photoelectrocatalytic oxidation of xylidine. These studies underline the importance of synthesizing new molecules and testing the catalytic efficiencies of novel materials. In addition, new experimental conditions and new AOP technologies need to be developed for the efficient, cost-effective oxidative mineralization of organic materials in polluted waters.

## Abbreviations list

AOP	Advanced Oxidation Processes
AOT	Advanced Oxidation Technologies
$\text{HO}^\bullet$	Hydroxyl Radical
$\text{SO}_4^{\bullet-}$	Sulfate Radical Anion
DHB	Dihydroxybenzene
CE	Chlorimurum-Ethyl
MTX	Mitoxantrone
$\text{K}_3(\text{FeOx})$	Potassium Ferrioxalate



SEM	Scanning Electron Microscopic
MV <sup>2+</sup>	Methyl Viologen
MB	Methylene Blue

## Acknowledgements

The authors acknowledge the Brazilian funding agencies CAPES, CNPq and FUNDECT for financial and fellowship support. F.H.Q. is associated with NAP-PhotoTech, the USP Research Consortium for Photochemical Technology, and INCT-Catalysis. A.M.Jr. is associated with NAP-PhotoTech and INCT-EMA.

## Author details

Amilcar Machulek Jr.<sup>1\*</sup>, Silvio C. Oliveira<sup>1</sup>, Marly E. Osugi<sup>2</sup>, Valdir S. Ferreira<sup>1</sup>, Frank H. Quina<sup>3</sup>, Renato F. Dantas<sup>4</sup>, Samuel L. Oliveira<sup>1</sup>, Gleison A. Casagrande<sup>5</sup>, Fauze J. Anaissi<sup>6</sup>, Volnir O. Silva<sup>3</sup>, Rodrigo P. Cavalcante<sup>1</sup>, Fabio Gozzi<sup>1</sup>, Dayana D. Ramos<sup>1</sup>, Ana P.P. da Rosa<sup>1</sup>, Ana P.F. Santos<sup>1</sup>, Douclasse C. de Castro<sup>1</sup> and Jéssica A. Nogueira<sup>1</sup>

\*Address all correspondence to: machulekjr@gmail.com

1 Center for Exact Sciences and Technology (CCET), Federal University of Mato Grosso do Sul-UFMS; Campo Grande, MS, Brazil

2 Institute of Chemistry, University of Brasília; Brasília, DF, Brazil

3 Institute of Chemistry and NAP-PhotoTech – USP; University of São Paulo-USP; São Paulo, SP, Brazil

4 Department of Chemical Engineering, Faculty of Chemistry, University of Barcelona; Barcelona, Spain

5 Faculty of Exact Sciences and Technology (FACET), Federal University of Grande Dourados-UFGD; Dourados, MS, Brazil

6 Department of Chemistry, State University of Centro-Oeste - UNICENTRO; Guarapuava, PR, Brazil

## References

- [1] Legrini, O, Oliveros, E, & Braun, A. M. Photochemical Processes for Water Treatment. *Chemical Reviews* (1993). , 93(2), 671-698.
- [2] Sonntag C von Advanced Oxidation Processes: Mechanistic Aspects. *Water Science & Technology* (2008). , 58(5), 1015-1021.
- [3] Matilainen, A, & Sillanpää, M. Removal of Natural Organic Matter from Drinking Water by Advanced Oxidation Processes. *Chemosphere* (2010). , 80(4), 351-365.
- [4] Bauer, R, & Fallmann, H. The Photo-Fenton Oxidation- a Cheap and Efficient Wastewater Treatment Method. *Research on Chemical Intermediates* (1997). , 23(4), 341-354.
- [5] Machulek Jr A Quina F.H., Gozzi F., Silva V.O., Friedrich L.C., Moraes J.E.F. Fundamental Mechanistic Studies of the Photo-Fenton Reaction for the Degradation of Organic Pollutants. In: Puzyn T., Mostrag-Szlichtyng A. (ed) *Organic Pollutants Ten Years After the Stockholm Convention- Environmental and Analytical Update*. Rijeka: InTech; (2012). , 271-292.
- [6] Pignatello, J. J, Oliveros, E, & Mackay, E. Advanced Oxidation Processes for Organic Contaminant Destruction Based on the Fenton Reaction and Related Chemistry [published erratum appears in *Critical Reviews in Environmental Science and Technology* 2007;37 273-275] *Critical Reviews in Environmental Science and Technology* (2006). , 36(1), 1-86.
- [7] Bossmann, S. H, Oliveros, E, Gob, S, Siegwart, S, & Dahlen, E. P. Payawan Jr L, Straub M, Worner M, Braun AM. New Evidence against Hydroxyl Radicals as Reactive Intermediates in the Thermal and Photochemically Enhanced Fenton Reactions. *Journal of Physical Chemistry A* (1998). , 102(28), 5542-5550.
- [8] Benitez, F. J, Beltran-heredia, J, Acero, J. L, & Rubio, F. J. Chemical Decomposition of Trichlorophenol by Ozone, Fenton's Reagent, and UV Radiation. *Industrial & Engineering Chemistry Research* (1999). , 2(4), 6.
- [9] Friedrich, L. C, Mendes, M. A, Silva, V. O, & Zanta, C. Machulek Jr A, Quina FH. Mechanistic Implications of Zinc(II) Ions on the Degradation of Phenol by the Fenton Reaction. *Journal of the Brazilian Chemical Society* (2012). , 23(7), 1372-1377.
- [10] Pontes RFF Moraes JE, Machulek Jr A, Pinto JM. A Mechanistic Kinetic Model for Phenol Degradation by the Fenton Process. *Journal of Hazardous Materials* (2010).
- [11] Zanta CLPS Friedrich LC, Machulek Jr A, Higa KM, Quina FH. Surfactant Degradation by a Catechol-Driven Fenton Reaction. *Journal of Hazardous Materials* (2010).
- [12] Bigda, R. J. Consider Fenton's Chemistry for Wastewater Treatment. *Chemical Engineering Progress* (1995). , 91(12), 62-66.

- [13] Hamilton, G. A, Friedman, J. P, & Campbell, P. M. The Hydroxylation of Anisole by Hydrogen Peroxide in the Presence of Catalytic Amounts of Ferric Ion and Catechol. Scope, Requirements and Kinetic Studies. *Journal of the American Chemical Society* (1966). , 88(22), 5266-5268.
- [14] Hamilton, G. A. Hanifin Jr JW, Friedman JP. The Hydroxylation of Anisole by Hydrogen Peroxide in the Presence of Catalytic Amounts of Ferric Ion and Catechol. Product studies, Mechanism, and Relation to Some Enzymic Reactions. *Journal of the American Chemical Society* (1966). , 88(22), 5269-5272.
- [15] Luna, A. J. Machulek Jr A, Chiavone-Filho O, Moraes JEF, Nascimento CAO. Photo-Fenton Oxidation of Phenol and Organochlorides (DCP and 2,4-D) in Aqueous Alkaline Medium with High Chloride Concentration. *Journal of Environmental Management* (2012). C) 10-17., 2, 4.
- [16] Machulek Jr AMoraes JEF, Okano LT, Silvério CA, Quina FH. Photolysis of Ferric Ion in the Presence of Sulfate or Chloride Ions: Implications for the Photo-Fenton Process. *Photochemical & Photobiological Sciences* (2009). , 8(7), 985-991.
- [17] Machulek Jr AMoraes JE, Vautier-Giongo C, Silverio CA, Friedrich LC, Nascimento CAO, Gonzales MC, Quina FH. Abatement of the Inhibitory Effect of Chloride Anions in the Photo-Fenton Process. *Environmental Science & Technology* (2007).
- [18] Augugliaro, V, Litter, M, Palmisano, L, & Soria, J. The Combination of Heterogeneous Photocatalysis with Chemical and Physical Operations: A Tool for Improving the Photoprocess Performance. *Journal of Photochemistry and Photobiology C: Photochemistry Reviews* (2006). , 7(4), 127-144.
- [19] Machulek Jr AGogritchiani E, Moraes JE, Quina FH, Oliveros E, Braun AM. Kinetic and Mechanistic Investigation of the Ozonolysis of 2,4-Xylidine (2,4-dimethyl-aniline) in Acid Aqueous Solution. *Separation and Purification Technology* (2009). , 67(2), 141-148.
- [20] Zhao, L, Ma, J, Sun, Z, Liu, Z, & Yang, Y. Experimental Study on Oxidative Decomposition of Nitrobenzene in Aqueous Solution by Honeycomb Ceramic-Catalyzed Ozonation. *Frontiers Environmental Science & Engineering in China* (2008). , 2(1), 44-50.
- [21] Kuns, A, Peralta-zamora, P, Moraes, S. G, & Duran, N. Novas Tendências no Tratamento de Efluentes Têxteis. *Química Nova* (2002). , 25(1), 78-82.
- [22] Lin, S. H, & Yeh, K. L. Looking to Treat Wastewater? Try Ozone. *Chemical Engineering* (1993). , 100(5), 112-116.
- [23] Esplugas, S. Curso técnico, de novembro, (1995). LRR-Universidad de Concepcion-Chile, Concepción, Chile., 8-10.

- [24] Pera-titus, M, Garcia-molina, V, Baños, M. A, Gimenez, J, & Esplugas, S. Degradation of Chlorophenols by Means of Advanced Oxidation Processes: a General Review. *Applied Catalysis B: Environmental* (2004). , 47(4), 219-256.
- [25] Straehelin, S, & Hoigné, J. Decomposition of Ozone in Water in the Presence of Organic Solutes Acting as Promoters and Inhibitors of Radical Chain Reactions. *Environmental Science & Technology* (1985). , 19(12), 1209-1212.
- [26] WHO Guidelines for Drinking-Water Quality [electronic resource]: incorporating 1st and 2nd addenda Recommendations. 3rd ed. Geneva, Switzerland, World Health Organization; (2008).
- [27] Alfano, O. M, Cabrera, M I, & Cassano, A. E. Photocatalytic Reactions Involving Hydroxyl Radical Attack. *Journal of Catalysis* (1997). , 172(2), 370-379.
- [28] Herrmann, J, Guillard, M, & Pichat, C. P. Heterogeneous Photocatalysis: an Emerging Technology for Water Treatment. *Catalysis Today* (1993).
- [29] Minero, C, Pelizzetti, E, Malato, S, & Blanco, J. Large Solar Plant Photocatalytic Water Decontamination: Effect of Operational Parameters. *Solar Energy* (1996). , 56(5), 421-428.
- [30] Quina, F. H, Nascimento, C. A. O, Teixeira, A. C. S. C, Guardani, R, & Lopez-gejo, J. Degradacion Fotoquímica de Compuestos Organicos de Origen Industrial. In: Nudelman. N. (ed) *Química Sustentable*. Santa Fe, Argentina: Universidad Nacional del Litoral; (2004). , 205-220.
- [31] Valente JPSAraujo AB, Bozano DF, Padilha PM, Florentino AO. Síntese e Caracterização Textural do Catalisador CeO<sub>2</sub>/TiO<sub>2</sub> Obtido via Sol-Gel: Fotocatálise do Composto Modelo Hidrogenoftalato de Potássio. *Eclética Química* (2005). , 30(4), 7-12.
- [32] Bockelmann, D, Weichgrebe, D, Goslich, R, & Bahnemann, D. Concentrating versus Non-Concentrating Reactors for Solar Water Detoxication. *Solar Energy Materials and Solar Cells* (1995).
- [33] Corminboeuf, C, Carnal, F, Weber, J, Chovelon, J-M, & Chermette, H. Photodegradation of Sulfonylurea Molecules: Analytical and Theoretical DFT Studies. *Journal of Physical Chemistry A* (2003). , 107(47), 10032-10038.
- [34] BrazilMinistério da Agricultura, Pecuária e Abastecimento-MAPA. Instrução Normativa nº 2 de 3 de Janeiro de 2008". *Diário Oficial da União* de 8 de Janeiro de 2008.; nº 5. Seção 1 (2008). , 5-9.
- [35] Turci, R, Sottani, C, Schierl, R, & Minoia, C. Validation Protocol and Analytical Quality in Biological Monitoring of Occupational Exposure to Antineoplastic Drugs. *Toxicology Letters* (2006).
- [36] Cavalcante, R. P, Sandim, L. R, & Bogo, D. Barbosa AMJ, Osugi ME, Blanco M, Oliveira SC, Matos MFC, Machulek Jr A, Ferreira VS. Application of Fenton, Photo-Fenton, Solar Photo-Fenton, and UV/H<sub>2</sub>O<sub>2</sub> to Degradation of the Antineoplastic Agent

- Mitoxantrone and Toxicological Evaluation. *Environmental Science and Pollution Research*, in press (DOI:10.1007/s11356-012-1110-y).
- [37] Safarzadeh-amiri, A, Bolton, J. R, & Cater, S. R. Ferrioxalate-Mediated Photodegradation of Organic Pollutants in Contaminated Water. *Water Research* (1997). , 31(4), 787-798.
  - [38] Chen, X, & Mao, S. S. Titanium Dioxide Nanomaterials: Synthesis, Properties, Modifications, and Applications. *Chemical Reviews* (2007). , 107(7), 2891-2959.
  - [39] Osugi, M. E, Umbuzeiro, G. A, & Anderson, M. A. Zandoni MVB. Degradation of Metallophthalocyanine Dye by Combined Processes of Electrochemistry and Photoelectrochemistry. *Electrochimica Acta* (2005).
  - [40] Osugi, M. E, & Umbuzeiro, G. A. Castro FJV, Zandoni MVB. Photoelectrocatalytic Oxidation of Remazol Turquoise Blue and Toxicological Assessment of its Oxidation Products. *Journal of Hazardous Materials* (2006). , 137(2), 871-877.
  - [41] Osugi, M. E, & Rajeshwar, K. Ferraz ERA, Oliveira DP, Araújo ÂR, Zandoni MVB. Comparison of Oxidation Efficiency of Disperse Dyes by Chemical and Photoelectrocatalytic Chlorination and Removal of Mutagenic Activity. *Electrochimica Acta* (2009). , 2009(54), 7-2086.
  - [42] Osugi, M. E. Zandoni MVB, Chenthamarakshan CR, Tacconi NR, Woldemariam GA, Mandal SS, Rajeshwar K. Toxicity Assessment and Degradation of Disperse Azo Dyes by Photoelectrocatalytic Oxidation on Ti/TiO<sub>2</sub> Nanotubular Array Electrodes. *Journal of Advanced Oxidation Technologies* (2008). , 11(3), 425-434.
  - [43] Docters, T, Chovelon, J. M, Hermann, J. M, & Deloume, J. P. Syntheses of TiO<sub>2</sub> Photocatalysts by the Molten Salts Method: Application to the Photocatalytic Degradation of Prosulfuron (R). *Applied Catalysis B: Environmental*, (2004). , 50(4), 219-226.
  - [44] Eisler, R. Eisler's Encyclopedia of Environmentally Hazardous Priority Chemicals. Elsevier; (2007).
  - [45] Tachikawa, T, Tojo, S, Fujitsuka, M, & Majima, T. Direct Observation of the One-Electron Reduction of Methyl Viologen Mediated by the CO<sub>2</sub> Radical Anion during TiO<sub>2</sub> Photocatalytic Reactions. *Langmuir* (2004). , 20(22), 9441-9444.
  - [46] Mohabansi, N. P, Patil, V. B, & Yenkie, N. A Comparative Study on Photodegradation of Methylene Blue Dye Effluent by Advanced Oxidation Process by Using TiO<sub>2</sub>/ZnO Photocatalyst. *Rasayan Journal of Chemistry* (2011). , 4(4), 814-819.
  - [47] Grimes, CA, Mor, GK, & Ti, . 2 Nanotube Arrays: Synthesis, Properties, and Applications. Springer; 2009.